



ELSEVIER

Comput. Methods Appl. Mech. Engrg. 191 (2002) 4927–4948

**Computer methods  
in applied  
mechanics and  
engineering**

www.elsevier.com/locate/cma

# Modeling uncertainty in steady state diffusion problems via generalized polynomial chaos

Dongbin Xiu, George Em Karniadakis \*

*Division of Applied Mathematics, Center for Fluid Mechanics, Brown University, Box 1966, 37 Manning street, Providence, RI 02912, USA*

Received 3 December 2001; received in revised form 4 June 2002

---

## Abstract

We present a generalized polynomial chaos algorithm for the solution of stochastic elliptic partial differential equations subject to uncertain inputs. In particular, we focus on the solution of the Poisson equation with random diffusivity, forcing and boundary conditions. The stochastic input and solution are represented spectrally by employing the orthogonal polynomial functionals from the Askey scheme, as a generalization of the original polynomial chaos idea of Wiener [Amer. J. Math. 60 (1938) 897]. A Galerkin projection in random space is applied to derive the equations in the weak form. The resulting set of deterministic equations for each random mode is solved iteratively by a block Gauss–Seidel iteration technique. Both discrete and continuous random distributions are considered, and convergence is verified in model problems and against Monte Carlo simulations.

© 2002 Elsevier Science B.V. All rights reserved.

*Keywords:* Uncertainty; Random diffusion; Polynomial chaos

---

## 1. Introduction

It has been common practice in engineering to analyze systems based on deterministic mathematical models with precisely defined input data. However, since such ideal situations are rarely encountered in practice, the need to address uncertainties is now clearly recognized, and there has been a growing interest in the applications of probabilistic methods [1–4].

The probabilistic methods in engineering can be broadly classified into two major categories: methods using a statistical approach and methods using a non-statistical approach. The statistical approach includes Monte Carlo simulation, stratified sampling, Latin hypercube sampling, etc. These methods involve sampling and estimation and in most cases are straightforward to apply. However, since the accuracy of the

---

\* Corresponding author. Fax: +1-401-863-3369.

E-mail address: [gk@cfm.brown.edu](mailto:gk@cfm.brown.edu) (G. Em Karniadakis).

sampling techniques depends on the sample size, in accordance with the ‘weak law of large number’, simulations can become prohibitively expensive, especially for the systems that are already complicated in the *deterministic* case. Thus, these methods are often used as the last resort and research effort has been made in developing the non-statistical methods.

The most popular non-statistical method is the perturbation method, where the random field is expanded via Taylor series around its mean and truncated at certain order. Typically, at most second-order expansion is employed because the system of equations becomes extremely complicated beyond second-order. This approach, also called the ‘second moment analysis’ [5–7], has been used extensively in various fields [8]. An inherent limitation of the perturbation method is that the uncertainties cannot be too large, i.e. variances of the random field cannot be too large compared with their mean values, e.g. typically less than 10% [5]. Also, higher-order statistics are not readily available for the second moment method. Another approach is the Neumann expansion, which is based on the inverse of the stochastic operator in a Neumann series. This method too is restricted to small uncertainties and attempts have been made to couple it with the Monte Carlo simulation to obtain more efficient algorithms [9,10].

Another methodology of the non-statistical type is to ‘discretize’ directly the random field. Ghanem and Spanos pioneered a *polynomial chaos* expansion method and have successfully applied it to various problems in mechanics [11]. The polynomial chaos expansion is based on the homogeneous chaos theory of Wiener [12] and is essentially a spectral expansion of the random variables. It allows high-order representation and promises fast convergence; coupled with Karhunen–Loeve (KL) decomposition for the input and Galerkin projection in random space, it results in computationally tractable algorithms for large engineering systems [13]. More efficient Monte Carlo algorithms can also be designed when combined with the chaos expansion technique [13,14]. More recently, a theoretical framework of discretizing the random field via the finite element approach, i.e., piecewise polynomials, was proposed in [15].

The classical polynomial chaos expansion is based on the *Hermite* polynomials in terms of *Gaussian* random variables. Although in theory, it converges to any  $L_2$  functionals in the random space [16], it achieves optimal convergence rate only for Gaussian and near Gaussian random fields [17], and does not readily apply to the random fields with *discrete* distribution. A more general framework, called the ‘generalized polynomial chaos’ or the ‘Askey-chaos’, was proposed in [17]. Here the polynomials are chosen from the hypergeometric polynomials of the Askey scheme [18], and the underlying random variables are not restricted to Gaussian random variables. Instead, the type of random variables are chosen according to the stochastic input and the weighting function of these random variables determines the type of orthogonal polynomials to be used as the basis in the random space. The convergence properties of different bases were studied in [17] and exponential convergence rate was demonstrated for model problems. In [19] the generalized polynomial chaos was applied to modeling uncertainties in incompressible flow and in [20] to flow-structure interaction problems.

The main objective of this paper is to give a broad algorithmic framework to solve stochastic elliptic partial differential equations based on the generalized polynomial chaos expansion. The class of problems we solve has the form

$$\begin{cases} \nabla \cdot [\kappa(x; \omega) \nabla u(x; \omega)] = f(x; \omega), & (x; \omega) \in D \times \Omega, \\ u(x; \omega) = g(x; \omega), & (x; \omega) \in \partial D \times \Omega, \end{cases} \quad (1)$$

where  $D$  is a bounded domain in  $\mathbb{R}^d$  ( $d = 1, 2, 3$ ) and  $\Omega$  is a probability space.  $f$ ,  $g$  and  $\kappa$  are  $\mathbb{R}$ -values functions on  $D \times \Omega$ . This can be considered as a model of steady state diffusion problems subject to internal (diffusivity  $\kappa$ ) and/or external (source term  $f$  and/or Dirichlet boundary condition  $g$ ) uncertainties. Babuška was among the first to study rigorously *existence* of solutions of the random Dirichlet problem [21]. Bécus and Cozzarelli studied the existence and properties of the general solution to (1), see [22–24]. Also, in [15] the problem subject to random diffusivity and/or random source terms was studied and existence and uniqueness of the solution in the finite element context, both in physical space and random space, were

addressed. From a different perspective, problems similar to (1) were studied via homogenization methods to evaluate the ‘effective diffusivity’ of random media [25].

In this paper, we solve the steady state diffusion problem (1) by generalized polynomial chaos expansion, where the uncertainties can be introduced through  $\kappa$ ,  $f$ , or  $g$ , or some combinations. It is worth noting that when both  $\kappa$  and  $u$  are random, it is not obvious how to give a mathematical meaning or justification to the product of two stochastic processes if they are not smooth. However, the product is well defined in terms of the chaos expansion by using the concept of Wick product and Kondratiev space [26,27].

In Section 2, we present the concept of the generalized polynomial chaos, and in section 3 we apply the expansion to the solution of the steady state diffusion problem. Numerical results are presented in Section 4, and we conclude the paper with a discussion.

## 2. The generalized polynomial chaos

In this section we introduce the generalized polynomial chaos expansion along with the KL decomposition, another classical technique for representing random processes. The KL decomposition can be used in some cases to represent efficiently the known stochastic fields, i.e., the stochastic inputs.

### 2.1. The Askey scheme

The *generalized hypergeometric series*  ${}_rF_s$  is defined by

$${}_rF_s(a_1, \dots, a_r; b_1, \dots, b_s; z) = \sum_{k=0}^{\infty} \frac{(a_1)_k \cdots (a_r)_k}{(b_1)_k \cdots (b_s)_k} \frac{z^k}{k!}, \tag{2}$$

where  $b_i \neq 0, -1, -2, \dots$  for  $i = \{1, \dots, s\}$  to ensure the denominator factors in the terms of the series are not zero. The *Pochhammer symbol*  $(a)_n$  defined as

$$(a)_n = \begin{cases} 1, & \text{if } n = 0, \\ a(a+1) \cdots (a+n-1), & \text{if } n = 1, 2, 3, \dots \end{cases} \tag{3}$$

If one of the numerator parameters  $a_i$ ,  $i = 1, \dots, r$  is a negative integer, say  $a_1 = -n$ , the hypergeometric series (2) terminates at the  $n$ th-term and becomes a hypergeometric polynomial in  $z$ .

The Askey scheme, which is represented as a tree structure in Fig. 1 (following [28]), classifies the hypergeometric orthogonal polynomials and indicates the limit relations between them. The ‘tree’ starts with the Wilson polynomials and the Racah polynomials on the top. The Wilson polynomials are continuous while the Racah polynomials are discrete. The lines connecting different polynomials denote the limit transition relationships between them; this implies that the polynomials at the lower end of the lines can be obtained by taking the limit of one of the parameters from their counterparts on the upper end. For example, the limit relation between Jacobi polynomials  $P_n^{(\alpha, \beta)}(x)$  and Hermite polynomials  $H_n(x)$  is

$$\lim_{\alpha \rightarrow \infty} \alpha^{-(1/2)n} P_n^{(\alpha, \alpha)}\left(\frac{x}{\sqrt{\alpha}}\right) = \frac{H_n(x)}{2^n n!},$$

and between Meixner polynomials  $M_n(x; \beta, c)$  and Charlier polynomials  $C_n(x; a)$  is

$$\lim_{\beta \rightarrow \infty} M_n\left(x; \beta, \frac{a}{\beta}\right) = C_n(x; a).$$

For a detailed account of definitions and properties of hypergeometric polynomials, see [18]; for the limit relations of Askey scheme, see [28,29].

The orthogonal polynomials associated with the generalized polynomial chaos, include:

- Hermite, Laguerre and Jacobi polynomials for continuous distributions;
- Charlier, Meixner, Krawtchouk and Hahn polynomials for discrete distributions.

2.2. The generalized polynomial chaos: Askey-chaos

The original polynomial chaos [12,30] employs the Hermite polynomials in the random space as the trial basis to expand the stochastic processes. Cameron and Martin proved that such expansion converges to any second-order processes in the  $L_2$  sense [16]. It can be seen from Fig. 1 that the Hermite polynomials are a subset of the Askey scheme. The generalized polynomial chaos, or the Askey-chaos, was proposed in [17,19,20] and employs more types of orthogonal polynomials from the Askey scheme. Convergence to second-order stochastic processes can be possibly obtained as a generalization of Cameron–Martin theorem [16].

The chaos expansion is essentially a representation of a function  $f \in L_2(\Omega)$  where  $\Omega$  is the properly defined probability space. We denote by  $\{\phi_k\}_{k=0}^\infty$  the orthogonal polynomials from the Askey scheme, which form an orthogonal basis in  $L_2(\mathbb{R}^n)$ .

A general second-order random process  $X(\omega)$  can be represented in the form

$$\begin{aligned}
 X(\omega) = & c_0 \Psi_0 + \sum_{i_1=1}^{\infty} c_{i_1} \Psi_1(\zeta_{i_1}(\theta)) + \sum_{i_1=1}^{\infty} \sum_{i_2=1}^{i_1} c_{i_1 i_2} \Psi_2(\zeta_{i_1}(\theta), \zeta_{i_2}(\theta)) \\
 & + \sum_{i_1=1}^{\infty} \sum_{i_2=1}^{i_1} \sum_{i_3=1}^{i_2} c_{i_1 i_2 i_3} \Psi_3(\zeta_{i_1}(\theta), \zeta_{i_2}(\theta), \zeta_{i_3}(\theta)) + \dots,
 \end{aligned}
 \tag{4}$$

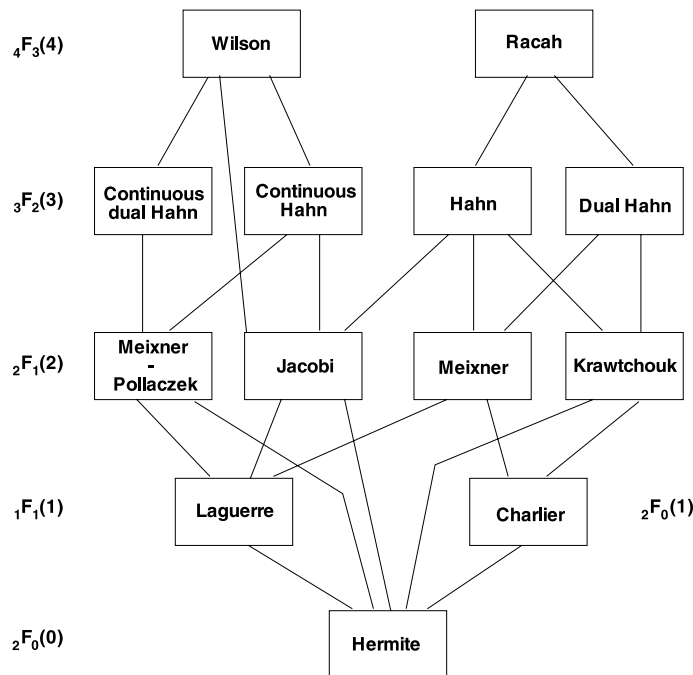


Fig. 1. The Askey scheme of orthogonal polynomials.

where  $\Psi_n(\xi_{i_1}, \dots, \xi_{i_n})$  denotes the generalized polynomial chaos of order  $n$  in terms of the multi-dimensional random variables  $\xi = (\xi_1, \dots, \xi_n, \dots)$ . Note that this is an infinite summation in the infinite dimensional space of  $\xi$ . The expansion bases  $\{\Psi_n\}$  are multi-dimensional hypergeometric polynomials defined as tensor-products of the corresponding one-dimensional polynomials bases  $\{\phi_k\}_{k=0}^\infty$ . Let  $\chi$  be the space of index sequences  $(\alpha_1, \alpha_2, \dots, \alpha_n, \dots) \in \mathbb{N}_0^{\mathbb{N}}$  and  $n := \sum_k \alpha_k$ . Then

$$\Psi_n(\xi_1, \xi_2, \dots, \xi_n) = \prod_{k=1}^n \phi_{\alpha_k}(\xi_k). \tag{5}$$

For notational and computational convenience, Eq. (4) is often rewritten, according to some numbering scheme, in the form with only one index as

$$X(\omega) = \sum_{j=0}^\infty a_j \Phi_j(\xi(\omega)), \tag{6}$$

where there is a one-to-one correspondence between the coefficients and basis functions in (4) and (6).

The family  $\{\Phi_n\}$  is an orthogonal basis in  $L_2(\Omega)$  with orthogonality relation

$$\langle \Phi_i, \Phi_j \rangle = \langle \Phi_i^2 \rangle \delta_{ij}, \tag{7}$$

where  $\delta_{ij}$  is the Kronecker delta and  $\langle \cdot, \cdot \rangle$  denotes the ensemble average which is the inner product in the Hilbert space of the variables  $\xi$

$$\langle f(\xi)g(\xi) \rangle = \int f(\xi)g(\xi)W(\xi) d\xi, \tag{8}$$

or

$$\langle f(\xi)g(\xi) \rangle = \sum_{\xi} f(\xi)g(\xi)W(\xi) \tag{9}$$

in the discrete case. Here  $W(\xi)$  is the weighting function corresponding to the Askey polynomials chaos basis  $\{\Phi_i\}$ .

In the original polynomial chaos,  $\{\Phi_n\}$  are the Hermite polynomials and  $\xi$  are the Gaussian random variables. In the Askey-chaos expansion, the orthogonal polynomials  $\{\Phi_n\}$  are not restricted to Hermite polynomials, instead they are determined by the weighting function of the corresponding random variables  $\xi$ , which are not necessarily Gaussian variables. The corresponding type of polynomials and their associated random variables are listed in Table 1. Since each type of polynomials from the Askey scheme form a complete basis in the Hilbert space determined by their corresponding support, we can expect each type of Askey-chaos to converge to any  $L_2$  functional in the  $L_2$  sense in the corresponding Hilbert functional space

Table 1  
Correspondence of the orthogonal polynomials and random variables for different Askey-chaos ( $N \geq 0$  is a finite integer)

	Random variables $\xi$	Orthogonal polynomials $\{\Phi_n\}$	Support
Continuous	Gaussian	Hermite	$(-\infty, \infty)$
	Gamma	Laguerre	$[0, \infty)$
	Beta	Jacobi	$[a, b]$
	Uniform	Legendre	$[a, b]$
Discrete	Poisson	Charlier	$\{0, 1, 2, \dots\}$
	Binomial	Krawtchouk	$\{0, 1, \dots, N\}$
	Negative Binomial	Meixner	$\{0, 1, 2, \dots\}$
	Hypergeometric	Hahn	$\{0, 1, \dots, N\}$

as a generalized result of the Cameron–Martin theorem [16,31]. Each type of orthogonal polynomials from the Askey-chaos has weighting functions of the same form as the probability function of its associated random variables  $\xi$ , as shown in Table 1.

The original polynomial chaos, the Hermite-chaos, is a subset of the continuous chaos and has been studied in the literature extensively. Here we show the Laguerre-chaos as another example of the *continuous chaos*. In one dimension, the  $n$ th-order Laguerre polynomials are defined as

$$L_n^{(a)}(\xi) = \frac{(-1)^n}{n!} e^{\xi} \xi^{-a} \left( \frac{d}{d\xi} \right)^n (e^{-\xi} \xi^{n+a}), \quad \xi > 0, \quad (10)$$

where parameter  $a > -1$  is a real positive number. The weight function in the orthogonality relation (7) is

$$W(\xi; a) = \frac{\xi^a e^{-\xi}}{\Gamma(a+1)}. \quad (11)$$

It can be seen that this is the same as the probability density function (PDF) of a Gamma random variable. The first few members of the one-dimensional Laguerre-chaos are:

$$\Phi_0 = 1, \quad \Phi_1 = \xi - (a+1), \quad \Phi_2 = \frac{1}{2!} \xi^2 - \xi(a+2) + \frac{1}{2}(a+1)(a+2), \dots \quad (12)$$

As an example of the *discrete chaos*, the Charlier-chaos employs the Charlier orthogonal polynomials as the basis in the random space. In one dimension, the  $n$ th-order Charlier polynomial can be written as

$$C_n(\xi; \lambda) = \lambda^n \sum_{r=0}^n (-1)^{n-r} \binom{n}{r} \frac{\xi^{(r)}}{\lambda^r}, \quad \xi = 0, 1, 2, \dots, \quad (13)$$

where  $\lambda > 0$  and  $\xi^{(r)} \equiv \xi(\xi-1)\dots(\xi-r+1)$ . The weighting function of Charlier polynomials is the probability function of the Poisson distribution with mean  $\lambda$

$$W(\xi; \lambda) = e^{-\lambda} \frac{\lambda^\xi}{\xi!}. \quad (14)$$

The first few members of the one-dimensional Charlier-chaos are:

$$\Phi_0 = 1, \quad \Phi_1 = \xi - 1, \quad \Phi_2 = \xi(\xi-1) - 2\lambda\xi + \lambda^2, \dots \quad (15)$$

### 2.3. The Karhunen–Loeve decomposition

The KL expansion is another way of representing a random process [32]. It is based on the spectral expansion of the correlation function of the process. It is particularly useful for the generalized polynomial chaos expansion as it provides a means of reducing the dimensionality of the random space. Let us denote the process by  $h(\mathbf{x}; \omega)$  and its correlation function by  $R_{hh}(\mathbf{x}, \mathbf{y})$ , where  $\mathbf{x}$  and  $\mathbf{y}$  are the spatial or temporal coordinates. By definition, the correlation function is real, symmetric, and positive definite. All eigenfunctions are mutually orthogonal and form a complete set spanning the function space to which  $h(\mathbf{x}; \omega)$  belongs. The KL expansion then takes the following form:

$$h(\mathbf{x}; \omega) = \bar{h}(\mathbf{x}) + \sum_{i=1}^{\infty} \sqrt{\lambda_i} \phi_i(\mathbf{x}) \xi_i(\omega), \quad (16)$$

where  $\bar{h}(\mathbf{x})$  denotes the mean of the random process, and  $\xi_i(\omega)$  forms a set of uncorrelated random variables. Also,  $\phi_i(\mathbf{x})$  and  $\lambda_i$  are the eigenfunctions and eigenvalues of the correlation function, respectively, i.e.,

$$\int R_{hh}(\mathbf{x}, \mathbf{y}) \phi_i(\mathbf{y}) \, d\mathbf{y} = \lambda_i \phi_i(\mathbf{x}). \tag{17}$$

Among other possible decompositions of a random process, the KL expansion is optimal in the sense that the mean-square error of the finite representation of the process is minimized. Its use, however, is limited as the correlation function of the solution process is often not known a priori. Nevertheless, the KL expansion provides an effective means of representing the input random processes when the correlation structure is known.

### 3. Galerkin projection

In this section we present the detailed algorithm for the application of the generalized polynomial chaos expansion to Eq. (1). By applying the chaos expansion, we expand the variables as

$$\kappa(x; \omega) = \sum_{i=0}^M \kappa_i(x) \Phi_i(\xi), \quad u(x; \omega) = \sum_{i=0}^M u_i(x) \Phi_i(\xi), \quad f(x; \omega) = \sum_{i=0}^M f_i(x) \Phi_i(\xi), \tag{18}$$

where we have replaced the infinite summation of  $\xi$  in infinite dimensions in Eq. (6) by a truncated finite-term summation of  $\{\Phi\}$  in the finite dimensions of  $\xi = (\xi_1, \dots, \xi_n)$ . The dimensionality  $n$  of  $\xi$  is determined by the random inputs. The random parameter  $\omega$  is absorbed into the polynomial basis  $\Phi(\xi)$ , thus the expansion coefficients  $\kappa_i$ ,  $u_i$  and  $f_i$  are deterministic. By substituting the expansion into governing equation (1), we obtain

$$\nabla \cdot \left[ \sum_{i=0}^M \kappa_i(x) \Phi_i \nabla \left( \sum_{j=0}^M u_j(x) \Phi_j \right) \right] = \sum_{i=0}^M f_i(x) \Phi_i. \tag{19}$$

Upon simplification, it can be written as

$$\sum_{i=0}^M \sum_{j=0}^M [\kappa_i(x) \nabla^2 u_j(x) + \nabla \kappa_i(x) \cdot \nabla u_j(x)] \Phi_i \Phi_j = \sum_{i=0}^M f_i(x) \Phi_i. \tag{20}$$

A Galerkin projection of the above equation onto each polynomial basis  $\{\Phi_i\}$  is then conducted in order to ensure that the error is orthogonal to the functional space spanned by the finite-dimensional basis  $\{\Phi_i\}$ . By projecting with  $\Phi_k$  for each  $k = \{0, \dots, M\}$  and employing the orthogonality relation (7), we obtain for each  $k = 0, \dots, M$ ,

$$\sum_{i=0}^M \sum_{j=0}^M [\kappa_i(x) \nabla^2 u_j(x) + \nabla \kappa_i(x) \cdot \nabla u_j(x)] e_{ijk} = f_k(x) \langle \Phi_k^2 \rangle, \tag{21}$$

where  $e_{ijk} = \langle \Phi_i \Phi_j \Phi_k \rangle$ . Together with  $\langle \Phi_i^2 \rangle$ , the coefficients  $e_{ijk}$  can be evaluated analytically from the definition of  $\Phi_i$ . By defining

$$b_{jk}(x) = \sum_{i=0}^M \kappa_i(x) e_{ijk}, \quad h_{jk}(x) = \sum_{i=0}^M \nabla \kappa_i(x) e_{ijk} = \nabla b_{jk}(x),$$

we can rewrite the above equation as

$$\sum_{j=0}^M [b_{jk}(x) \nabla^2 u_j(x) + h_{jk}(x) \cdot \nabla u_j(x)] = f_k(x) \langle \Phi_k^2 \rangle, \quad \forall k \in [0, M]. \tag{22}$$

Eq. (22) is a set of  $(M + 1)$  coupled elliptic partial differential equations. These equations are deterministic and can be solved by any conventional method, e.g., finite elements. In this paper we employ the spectral/*hp* element method [33]. The total number of equations  $(M + 1)$  is determined by the dimensionality of the chaos expansion  $(n)$  and the highest order  $(p)$  of the polynomials  $\{\Phi\}$ , where

$$(M + 1) = (n + p)! / (n!p!). \quad (23)$$

While it is possible to solve Eq. (22) via a direct solver, we choose to use an iterative method to take advantage of the diagonal dominance of the block matrix  $B = \{b_{jk}\}$ . In particular, we employ the block Gauss–Seidel iteration in the following form: for all  $k = 0, \dots, M$ ,

$$b_{kk}(x)\nabla^2 u_k^{n+1}(x) + h_{kk}(x) \cdot \nabla u_k^{n+1}(x) = f_k(x)\langle \Phi_k^2 \rangle - \sum_{j=0}^{k-1} [b_{jk}(x)\nabla^2 u_j^{n+1}(x) + h_{jk}(x) \cdot \nabla u_j^{n+1}(x)] - \sum_{j=k+1}^M [b_{jk}(x)\nabla^2 u_j^n(x) + h_{jk}(x) \cdot \nabla u_j^n(x)], \quad (24)$$

where the superscript  $n$  denotes the iteration number. The convergence criterion is defined as

$$\frac{\|u_k^{n+1}(x) - u_k^n(x)\|}{\|u_k^1(x) - u_k^0(x)\|} \leq \varepsilon, \quad \forall k \in [0, M], \quad (25)$$

where  $\varepsilon$  is a small positive number and different types of norm  $\|\cdot\|$  can be used. In this paper the  $L_\infty$  norm is used and  $\varepsilon$  is set to be  $10^{-5}$ – $10^{-7}$ . For all the results we present here, the block Gauss–Seidel iteration normally converges within about 10 steps. A similar iteration technique was used in [34] for stochastic modeling of elasto-plastic body problems with the Hermite-chaos and fast convergence was reported too.

#### 4. Numerical results

In this section we present numerical results of the proposed generalized polynomial chaos expansion to stochastic diffusion problem. We first consider an one-dimensional model problem where the exact solution is available; then a more complicated two-dimensional problem where we use Monte Carlo simulation to validate the chaos solution. Among the types of chaos expansions listed in Table 1, we choose two continuous chaos: Hermite-chaos and Jacobi-chaos; and two discrete chaos: Charlier-chaos and Krawtchouk-chaos for demonstration purposes. Finally, we solve the random heat conduction problem in a grooved channel as an example of a more practical application.

##### 4.1. One-dimensional model problem

Consider the following problem

$$\frac{d}{dx} \left[ \kappa(x; \omega) \frac{du}{dx}(x; \omega) \right] = 0, \quad x \in [0, 1], \quad (26)$$

with boundary conditions

$$u(0; \omega) = 0, \quad u(1; \omega) = 1.$$

The random diffusivity has the form

$$\kappa(x; \omega) = 1 + \epsilon(\omega)x, \quad (27)$$

where  $\epsilon(\omega)$  is a random variable, and  $\kappa(x; \omega) > 0$ . The exact solution to this problem is

$$u_e(x; \omega) = \begin{cases} \ln[1 + \epsilon(\omega)x] / \ln[1 + \epsilon(\omega)], & \text{for } \epsilon(\omega) \neq 0; \\ x, & \text{for } \epsilon(\omega) = 0. \end{cases} \tag{28}$$

The ‘mean-square’ error of the numerical solution from the generalized chaos expansion  $u_p(x, \omega)$  is computed

$$e_2(x) = \left( \mathbb{E}[u_p(x, \omega) - u_e(x, \omega)]^2 \right)^{1/2},$$

where  $\mathbb{E}$  denotes the ‘expectation’ operator and  $p$  is the order of the chaos expansion. Specifically, we examine the ‘mean-square’ convergence ( $L_2$  convergence in random space) of the  $L_\infty$  norm (in physical space) of  $e_2(x)$  as  $p$  increases.

4.1.1. Jacobi-chaos and beta distribution

We assume  $\epsilon(\omega)$  in Eq. (27) is a Beta random variable, i.e., its PDF has the form

$$f(\epsilon; \alpha, \beta) = \frac{(1 - \epsilon)^\alpha (1 + \epsilon)^\beta}{2^{\alpha+\beta+1} B(\alpha + 1, \beta + 1)}, \quad \epsilon \in [-1, 1], \quad \alpha, \beta > -1, \tag{29}$$

where  $B(\alpha, \beta)$  is the  $\beta$  function defined as  $B(p, q) = \Gamma(p)\Gamma(q)/\Gamma(p + q)$ . The corresponding generalized polynomial chaos, according to Table 1, is the Jacobi-chaos. An important special case is when  $\alpha = \beta = 0$ , then  $\epsilon(\omega)$  becomes an *uniform* random variable and the corresponding chaos becomes the Legendre-chaos (see Table 1).

In Fig. 2 the mean-square convergence of the Jacobi-chaos solution is shown with different standard deviation  $\sigma$  of the input as a measure of the magnitude of the input uncertainty. It can be seen on the semi-log scale that the Jacobi-chaos solution, including the Legendre-chaos for uniform random variables, converges exponentially fast as the expansion order  $p$  increases. The exponential convergence rate is retained for large input uncertainty such as  $\sigma = 0.9$ , which is close to the limit of the existence of the solution ( $\sigma < 1$ ). This is in contrast to the perturbation-based method which normally works for  $\sigma < 0.1$ .

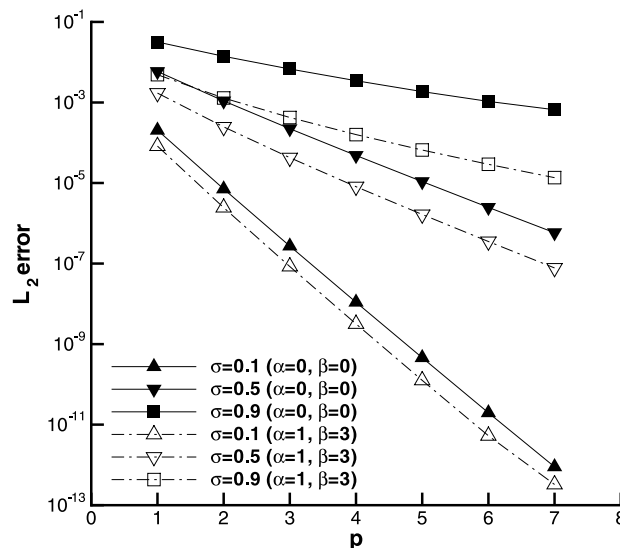


Fig. 2. Convergence of Jacobi-chaos for the one-dimensional model problem.

#### 4.1.2. Hermite-chaos and Gaussian distribution

We now assume  $\epsilon(\omega)$  in Eq. (27) is a Gaussian random variable with PDF

$$f(\epsilon) = \frac{1}{\sqrt{2\pi}} e^{-\epsilon^2/2}, \quad \epsilon \in (-\infty, \infty). \quad (30)$$

The corresponding generalized polynomial chaos is the Hermite-chaos (Table 1).

While the random input has infinite support and rigorous analysis of the existence and uniqueness of the solution is lacking to ensure  $\kappa(x, \omega) > 0$  in Eq. (27) in some stochastic sense, it is intuitive to assume that the solution exists for random input with small deviation  $\sigma$ . In this paper, we assume  $\sigma = 0.1$  and the mean-square convergence of the Hermite-chaos solution is shown in Fig. 3. Again, exponential convergence rate is achieved.

#### 4.1.3. Charlier-chaos and Poisson distribution

We now assume  $\epsilon(\omega)$  in Eq. (27) is a discrete random variable with Poisson distribution

$$f(\epsilon; \lambda) = e^{-\lambda} \frac{\lambda^\epsilon}{\epsilon!}, \quad \epsilon = 0, 1, 2, \dots, \lambda > 0. \quad (31)$$

The corresponding generalized polynomial chaos is the Charlier-chaos (Table 1). Again we assume relatively small deviation  $\sigma = 0.1$  to ensure the existence of the solution. The exponential convergence of the Charlier-chaos expansion is shown in Fig. 4 for two different values of the parameter  $\lambda$ .

#### 4.1.4. Krawtchouk-chaos and binomial distribution

In this section  $\epsilon(\omega)$  in Eq. (27) is assumed to be a discrete random variable with binomial distribution

$$f(\epsilon; p, N) = \binom{N}{\epsilon} q^\epsilon (1-q)^{N-\epsilon}, \quad 0 \leq q \leq 1, \quad \epsilon = 0, 1, \dots, N. \quad (32)$$

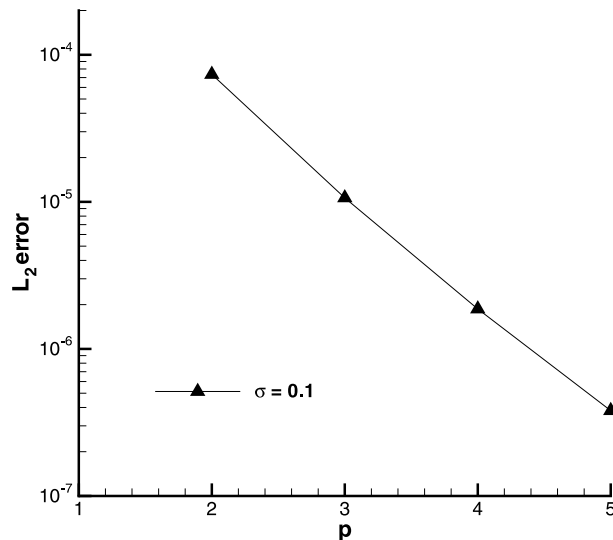


Fig. 3. Convergence of Hermite-chaos for the one-dimensional model problem.

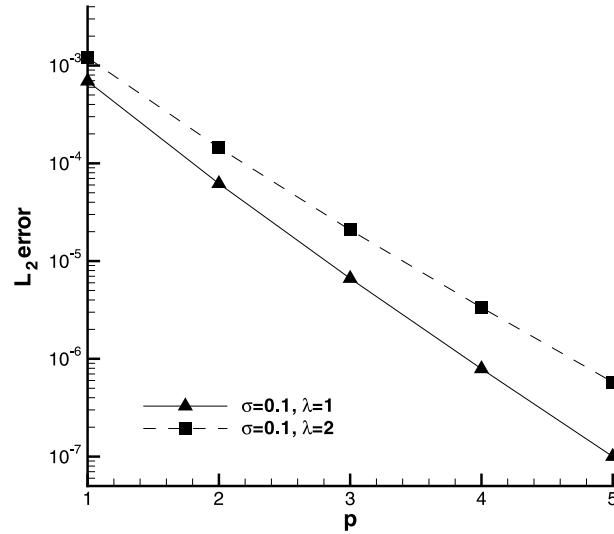


Fig. 4. Convergence of Charlier-chaos for the one-dimensional model problem.

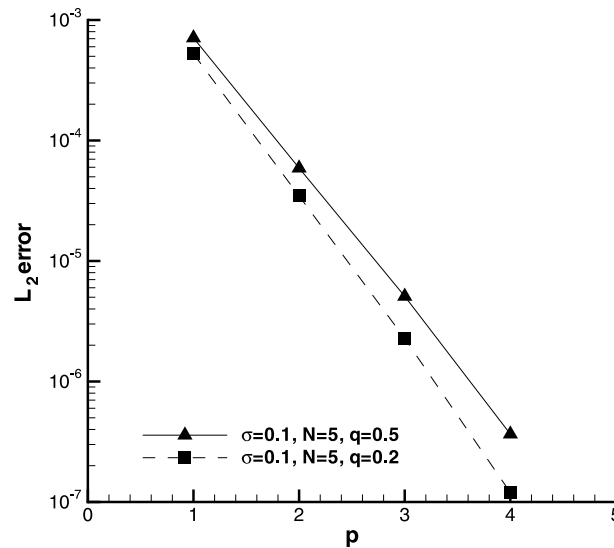


Fig. 5. Convergence of Krawtchouk-chaos for the one-dimensional model problem.

The corresponding generalized polynomial chaos is the Krawtchouk-chaos (Table 1). Exponential convergence of the Krawtchouk-chaos expansion can be seen in Fig. 5 with different values of the parameters ( $N, q$ ).

#### 4.2. Two-dimensional model problem

In this section we consider the two-dimensional problem

$$\nabla \cdot [\kappa(x, y; \omega) \nabla u(x, y; \omega)] = f(x, y; \omega), \quad (x, y) \in [-1, 1] \times [-1, 1], \tag{33}$$

with boundary conditions

$$u(-1, y; \omega) = 1, \quad \frac{\partial u}{\partial x}(1, y; \omega) = 0, \quad u(x, -1; \omega) = 0, \quad \frac{\partial u}{\partial y}(x, 1; \omega) = 0.$$

The diffusivity  $\kappa(x, y; \omega)$  and source term  $f(x, y; \omega)$  are stochastic processes with certain distribution and given correlation function  $C(x_1, y_1; x_2, y_2)$ . The mean fields are:  $\bar{\kappa}(x, y; \omega) = 1$  and  $\bar{f}(x, y; \omega) = 0$ . The KL decomposition is applied to the correlation function to reduce the dimensionality in the random space; the generalized polynomial chaos expansion is then applied to the solution.

#### 4.2.1. The Bessel correlation function

The most commonly used correlation function for stochastic processes is the *exponential* function. In the one-dimensional case, it takes the form

$$C(x_1, x_2) = e^{-|x_1 - x_2|/b}, \quad (34)$$

where  $b$  is the correlation length. This correlation function is the result of first-order autoregression

$$\xi_t = a\xi_{t-1} + \epsilon_t, \quad a > 0, \quad (35)$$

where  $\xi_t$  is the random series at  $t = \dots, -2, -1, 0, 1, 2, \dots$  and  $\epsilon_t$  is an independent identically distributed random series. This is a *unilateral* type of scheme where the dependence is extended only in one direction, and it is the simplest realistic *time series*. For *space series*, a *bilateral* autoregression is more realistic

$$\xi_t = a\xi_{t-1} + b\xi_{t+1} + \epsilon_t, \quad (36)$$

where it is intuitively clear that  $a$  and  $b$  cannot be too large. It is shown that the bilateral type of scheme is not necessary in one dimension as it can be effectively reduced to a unilateral one [35]. Thus the exponential correlation function can be considered as the ‘elementary’ correlation in one dimension. It has been used extensively in the literature and its KL decomposition can be solved analytically [11].

In two dimensions, the exponential correlation function can be written as  $C(r) = e^{-r/b}$  where  $r$  is the distance between two spatial points. This function has been also used in the literature. However, as Whittle pointed out in [35], it is necessary to introduce autoregression schemes with dependence in all directions for more realistic models of random series in *space*. The simplest such model is

$$\xi_{st} = a(\xi_{s+1,t} + \xi_{s-1,t} + \xi_{s,t+1} + \xi_{s,t-1}) + \epsilon_{st}, \quad (37)$$

where  $\xi_{st}$  is random field at grid  $(s, t)$  and  $\epsilon_{st}$  is independent identically distributed random field. This model corresponds to a stochastic Laplace equation in the continuous case:

$$\left[ \left( \frac{\partial}{\partial x} \right)^2 + \left( \frac{\partial}{\partial y} \right)^2 - \frac{1}{b^2} \right] \xi(x, y) = \epsilon(x, y), \quad (38)$$

where  $1/b^2 = 1/a - 4$ . The ‘elementary’ correlation function in two dimensions can be solved from the above equation:

$$C(r) = \frac{r}{b} K_1 \left( \frac{r}{b} \right), \quad (39)$$

where  $K_1$  is the modified Bessel function of the second kind with order 1,  $b$  scales as the correlation length and  $r$  is the distance between two points. On the other hand, the exponential correlation function  $C(r) = e^{-r/b}$  in two dimensions corresponds to a rather artificial system

$$\left[ \left( \frac{\partial}{\partial x} \right)^2 + \left( \frac{\partial}{\partial y} \right)^2 - \frac{1}{b^2} \right]^{3/4} \zeta(x, y) = \epsilon(x, y). \tag{40}$$

It is difficult to visualize a physical mechanism which would lead to such a relation. For a detailed discussion on this subject, see [35].

In this paper, we employ (39) as the correlation function of  $\kappa$  and  $f$ . Since no analytical solution is available for the eigenvalue problem (17) of the KL decomposition for this correlation function, a numerical eigenvalue solver is employed. Fig. 6 shows the distribution of the first 20 eigenvalues. Here the

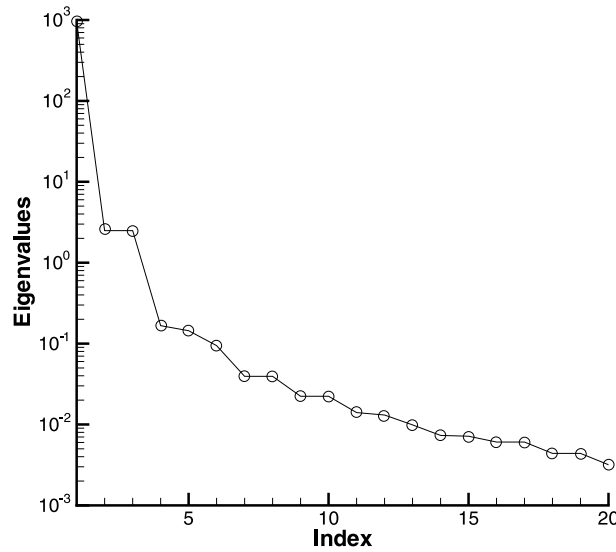


Fig. 6. Eigenvalues of KL decomposition with Bessel correlation function (39),  $b = 20$ .

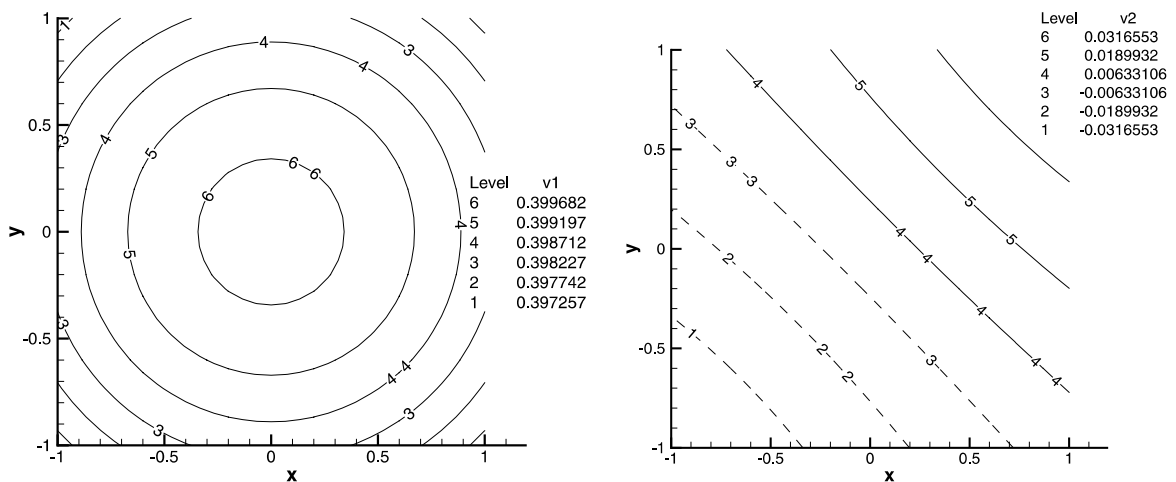


Fig. 7. Eigenfunctions of the KL decomposition with the Bessel correlation function (39),  $b = 20$ ; left: first eigenfunction, right: second eigenfunction (dashed lines denote negative values).

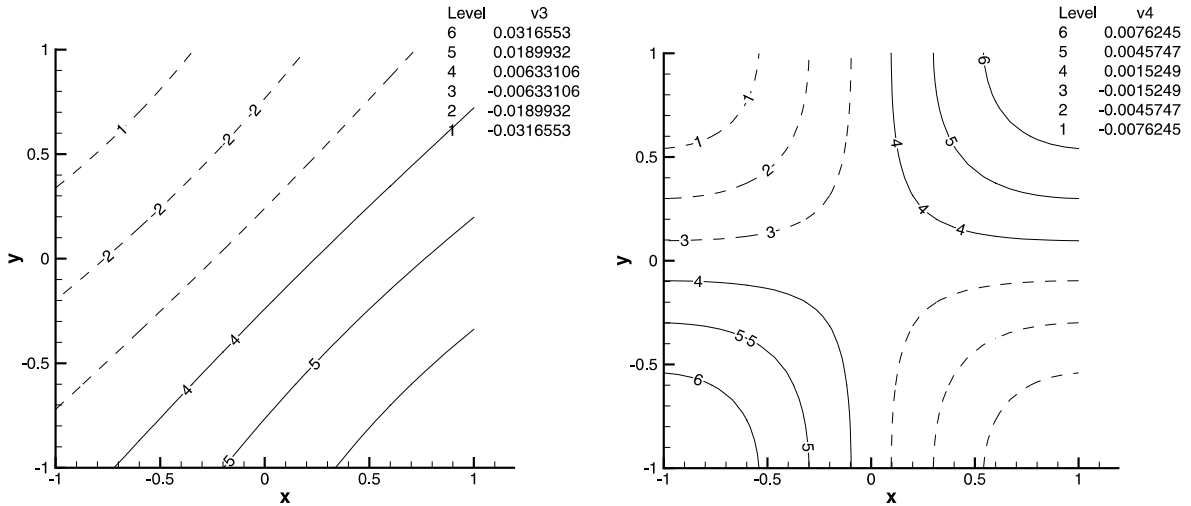


Fig. 8. Eigenfunctions of the KL decomposition with the Bessel correlation function (39),  $b = 20$ ; left: third eigenfunction, right: fourth eigenfunction (dashed lines denote negative values).

parameter  $b$  is set to  $b = 20$ . In Figs. 7 and 8 the eigenfunctions corresponding to the first four eigenvalues are plotted.

#### 4.2.2. Legendre-chaos and uniform distribution

In this section we assume  $\kappa(x, y; \omega)$  and  $f(x, y; \omega)$  are random fields resulted from the KL decomposition (16) of the Bessel correlation function (39), and with the underlying random variables having uniform distributions. For computational simplicity, we further assume  $k$  and  $f$  are fully cross-correlated. Due to the fast decay of eigenvalues as shown in Fig. 6, we choose the first four eigenmodes from the KL decomposition. This results in a four-dimensional (in random space) chaos expansion. The corresponding chaos in this case is the Legendre-chaos (Table 1).

The spectral/ $hp$  element method is used for spatial discretization. For detailed account of spectral/ $hp$  element method, see [33]. Specifically, an array of  $5 \times 5$  elements are used in the domain and sixth-order polynomials are employed as the (spatial) expansion basis in each element.<sup>1</sup> Numerical tests show that this is sufficient to resolve the solution in space. The standard deviations of the random inputs are  $\sigma_\kappa = \sigma_f = 0.4$ . Resolution checks in random space were conducted, and it was shown that third-order ( $p = 3$ ) Legendre-chaos results in converged solution. For four-dimensional chaos ( $n = 4$ ), the total number of expansion terms is 35 (see Eq. (23)).

Since no analytical solution is available, we employ Monte Carlo simulations to validate the chaos solution. Here we conduct the Monte Carlo computation *after* the KL decomposition, i.e., we generate the random number ensemble on the reduced basis from the KL decomposition. In this way the error from generalized polynomial chaos expansion is isolated, while the error introduced by the finite-term truncation of KL decomposition, which is well understood, is excluded.

The solution profile along the horizontal centerline through the domain is considered in Fig. 9. The mean solution of Legendre-chaos and Monte Carlo simulation with different number of realizations are shown, together with the corresponding deterministic solution. A noticeable difference between the stochastic mean

<sup>1</sup> We note here that the Jacobi polynomials of mixed weights are used in the spectral/ $hp$  element method.

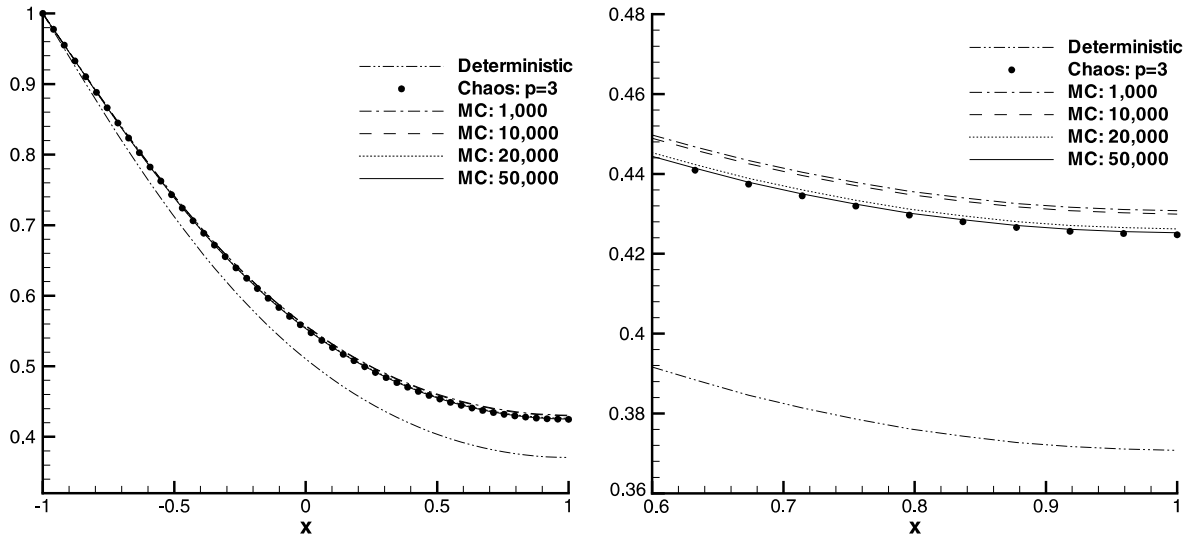


Fig. 9. Two-dimensional model problem: uniform random distribution and Legendre-chaos; left: mean solution along the horizontal centerline, right: close-up view.

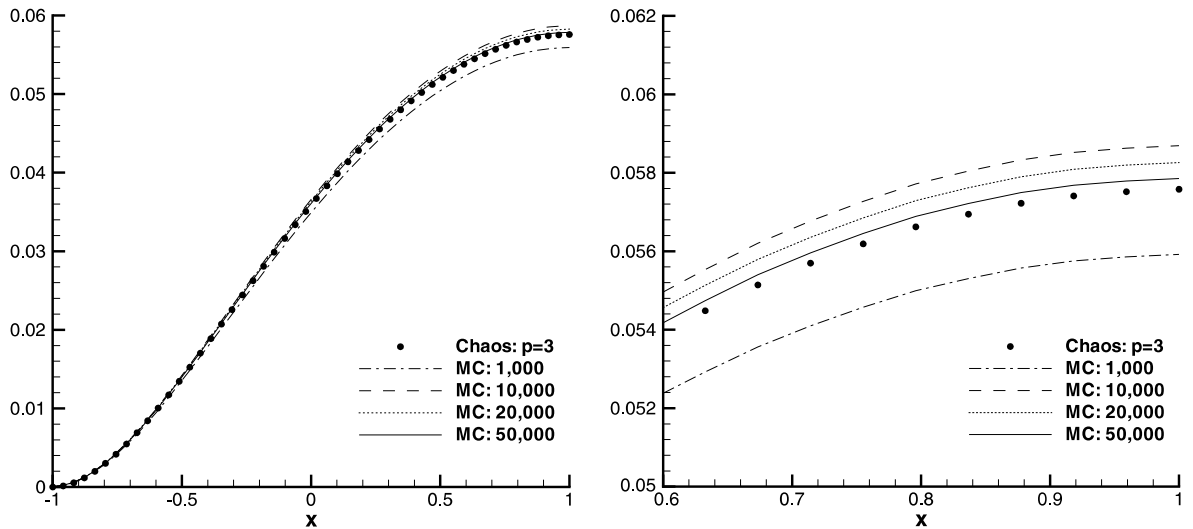


Fig. 10. Two-dimensional model problem: uniform random distribution and Legendre-chaos; left: variance along the horizontal centerline, right: close-up view.

profile and the deterministic profile is observed. In Fig. 10 the variance of the stochastic solution along the horizontal centerline is shown. It is seen that the Monte Carlo solution converges to the chaos solution as the number of realizations increases. Good agreement is obtained with 50,000 realizations.

Similar results are obtained for other solution profiles in the domain, for example, the vertical centerline.

4.2.3. Hermite-chaos and Gaussian distribution

We now assume the random field  $\kappa(x, y; \omega)$  and  $f(x, y; \omega)$  are Gaussian processes with  $\sigma_\kappa = \sigma_f = 0.2$ . All the remaining parameters are the same as the above example. The corresponding generalized polynomial chaos is the Hermite-chaos.

The same solution profiles along the horizontal centerline of the domain are shown in Figs. 11 and 12, for the mean solution and the variance, respectively. In this case, a fourth-order Hermite-chaos ( $p = 4$ ) is

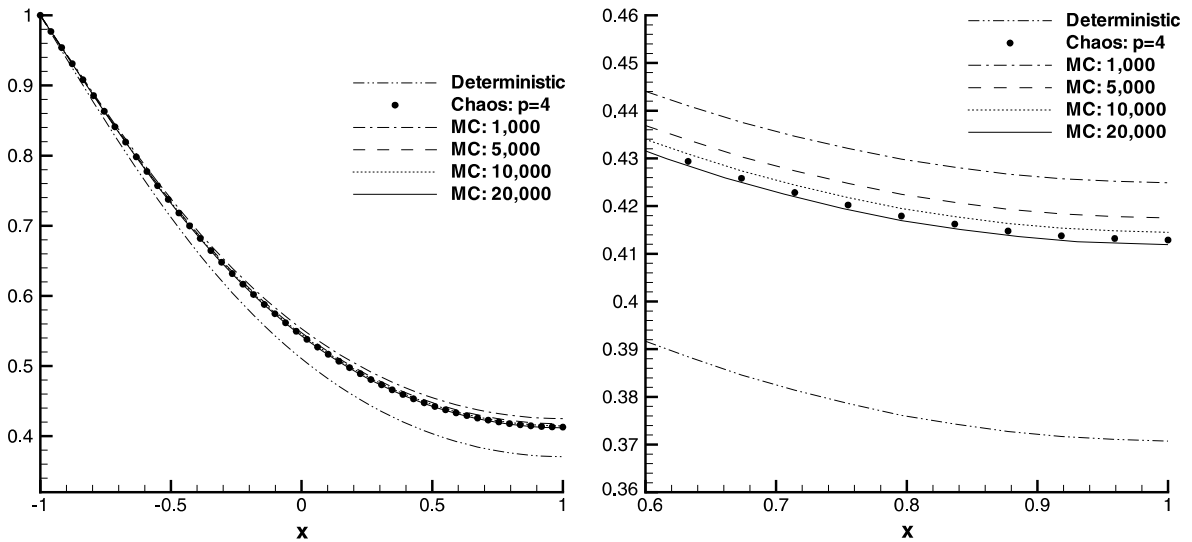


Fig. 11. Two-dimensional model problem: Gaussian random distribution and Hermite-chaos; left: mean solution along the horizontal centerline, right: close-up view.

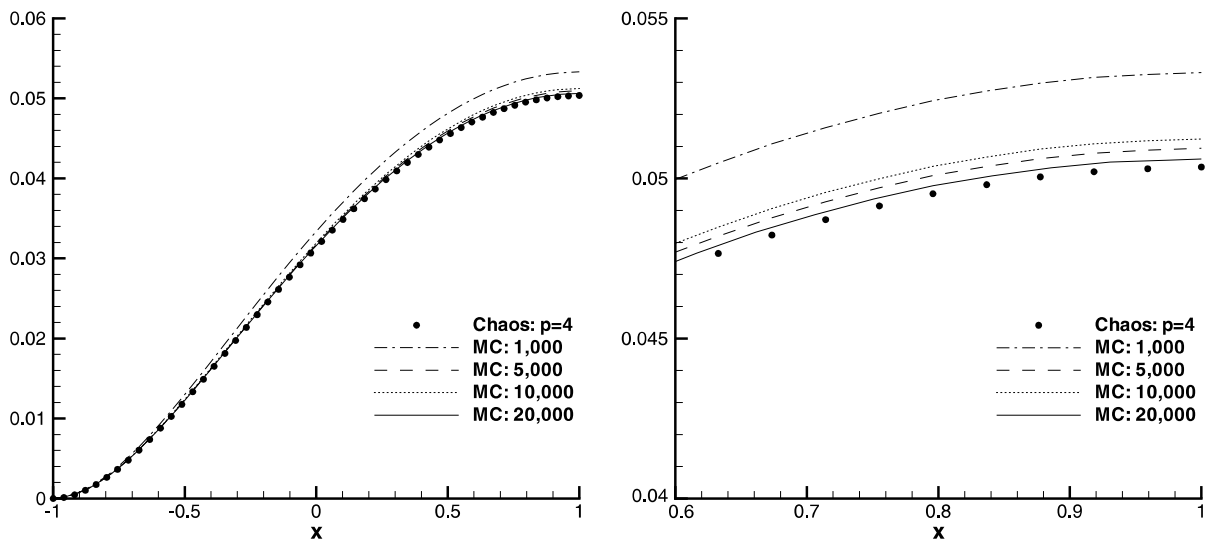


Fig. 12. Two-dimensional model problem: Gaussian random distribution and Hermite-chaos; left: variance along the horizontal centerline, right: close-up view.

required to obtain converged result in random space. This corresponds to a 70-term expansion from formula (23) for  $n = 4, p = 4$ . The corresponding solution of the Monte Carlo simulation converges relatively fast in this case, and for 20,000 realizations it converges to the Hermite-chaos solution.

4.2.4. Charlier-chaos and Poisson distribution

As an example of the discretely distributed random fields, we now assume the diffusivity  $\kappa(x, y; \omega)$  and source term  $f(x, y; \omega)$  are processes resulted from Poisson random variables in the KL decomposition (16), with  $\sigma_\kappa = \sigma_f = 0.2$ . The parameter  $\lambda = 1$  as in Eq. (31).

The third-order ( $p = 3$ ) corresponding generalized chaos, the Charlier-chaos, results in resolution-independent solution in random space. The Monte Carlo solution converges to the solution of Charlier-chaos; with 100,000 realizations we obtain good agreement. The solution profiles of the mean and variance along the horizontal centerline are shown in Figs. 13 and 14, respectively.

4.2.5. Krawtchouk-chaos and binomial distribution

Finally, the random field of  $\kappa(x, y; \omega)$  and  $f(x, y; \omega)$  are assumed to have the binomial distributed random variables with ( $N = 5, q = 0.5$ ) from Eq. (32) in their KL expansion. The standard deviations are  $\sigma_\kappa = \sigma_f = 0.2$ .

Fig. 15 shows the mean solution along the horizontal centerline of the domain, while Fig. 16 shows the variance profile. The third-order ( $p = 3$ ) Krawtchouk-chaos is sufficient to resolve the problem in random space. On the other hand, the solution of Monte Carlo simulation converges to the chaos solution with 50,000 realizations.

4.3. Random heat conduction in a grooved channel

In this section we consider the steady state heat conduction in a grooved channel subject to uncertainties in boundary conditions and diffusivity.

$$\nabla \cdot [\kappa(x, y; \omega) \nabla u(x, y; \omega)] = 0, \quad (x, y) \in D, \tag{41}$$

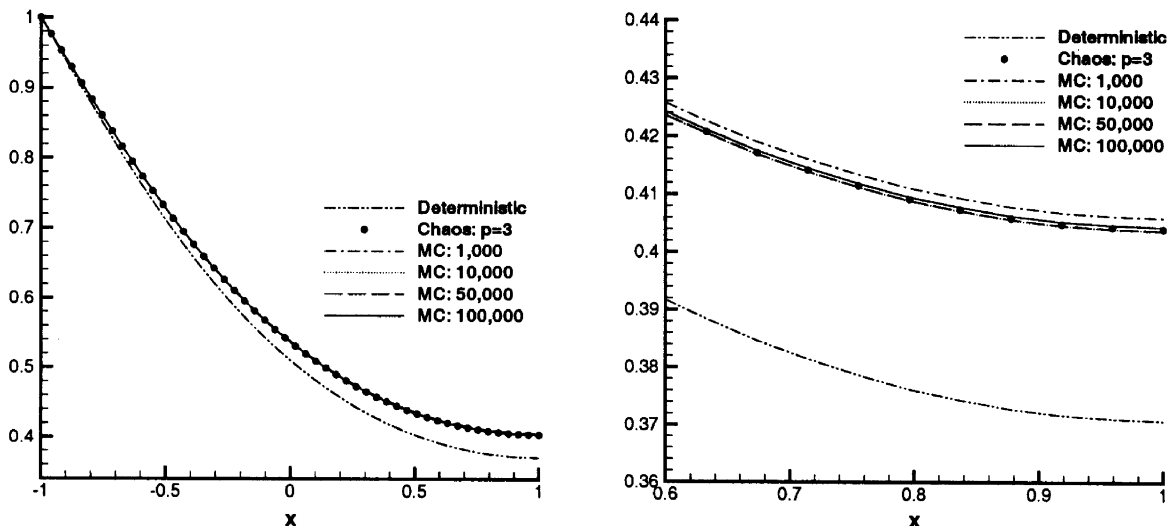


Fig. 13. Two-dimensional model problem: Poisson random distribution and Charlier-chaos; left: mean solution along the horizontal centerline, right: close-up view.

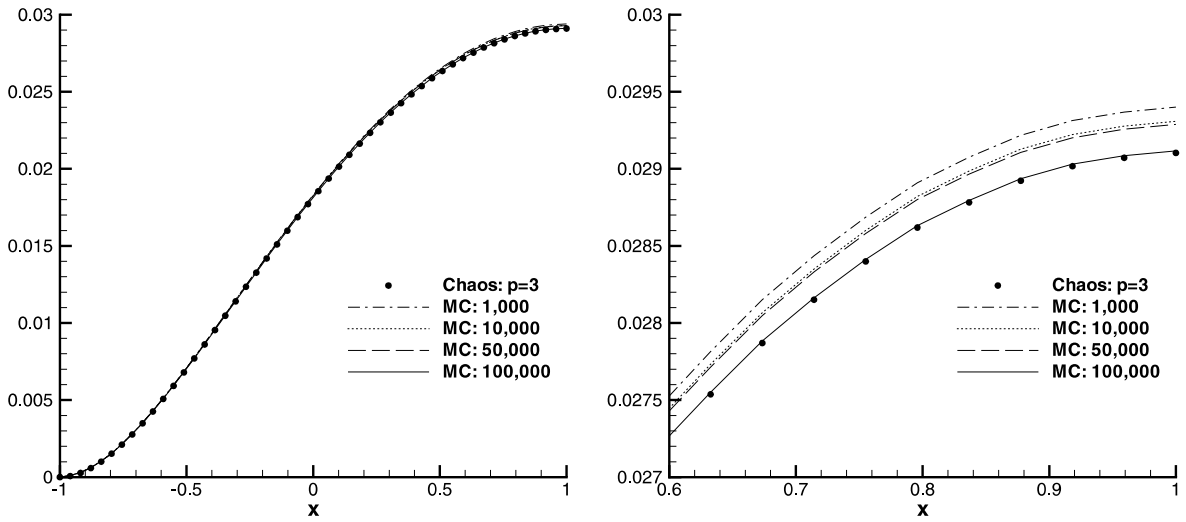


Fig. 14. Two-dimensional model problem: Poisson random distribution and Charlier-chaos; left: variance along the horizontal centerline, right: close-up view.

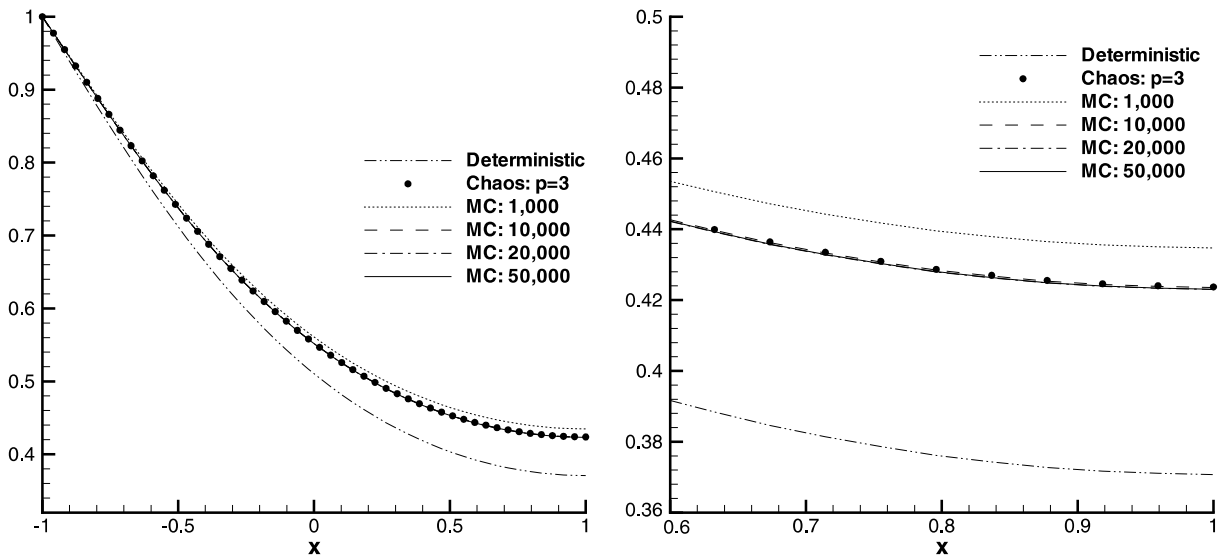


Fig. 15. Two-dimensional model problem: binomial random distribution and Krawtchouk-chaos; left: mean solution along the horizontal centerline, right: close-up view.

where the computational domain  $D$  is shown in Fig. 17. The boundary of the domain consists of four segments: the top of the channel  $\Gamma_T$ , the bottom of the channel  $\Gamma_B$ , the two sides of the channel  $\Gamma_S$  and the boundaries of the cavity  $\Gamma_C$ . The diffusivity  $\kappa(x, y; \omega)$  is a random field with uniformly distributed random variables in its KL decomposition, with mean field  $\bar{\kappa}(x, y; \omega) = 1$  and the same Bessel correlation function as in Section 4.2.1. The boundary conditions are

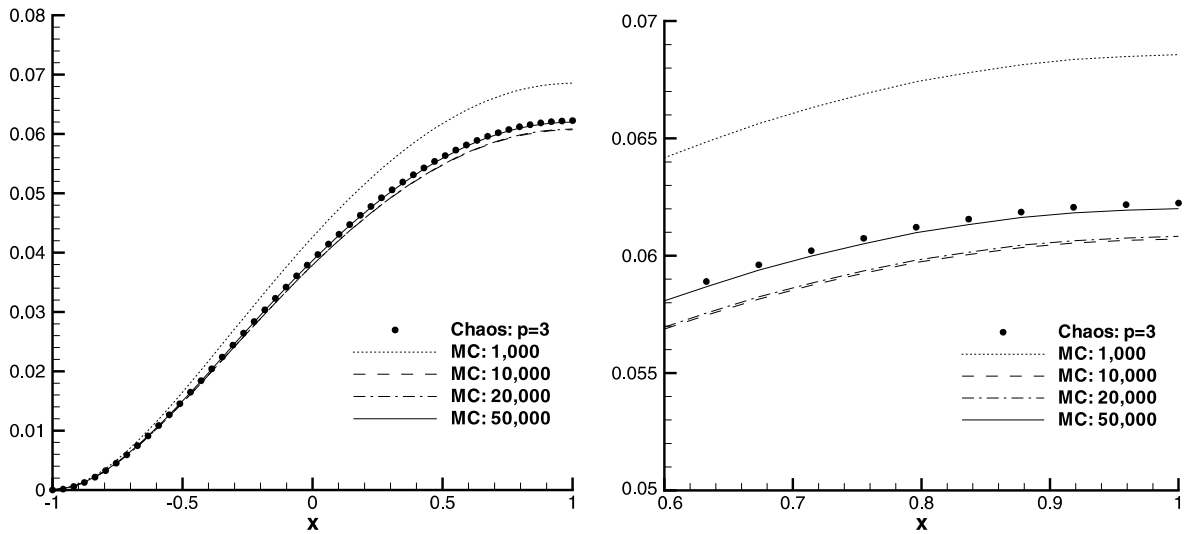


Fig. 16. Two-dimensional model problem: binomial random distribution and Krawtchouk-chaos; left: variance along the horizontal centerline, right: close-up view.

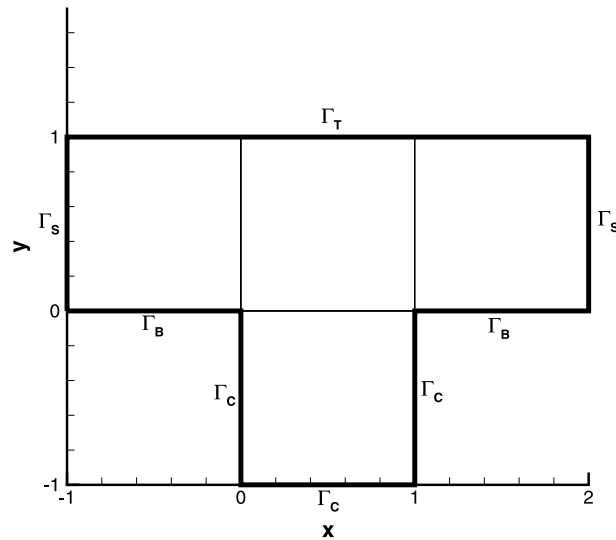


Fig. 17. Schematic of the domain of the grooved channel.

$$u|_{\Gamma_T} = 0, \quad u|_{\Gamma_B} = 1, \quad \left. \frac{\partial u}{\partial x} \right|_{\Gamma_S} = 0, \quad u|_{\Gamma_C} = 1 + \xi, \quad (42)$$

where  $\xi$  is a random variable with uniform distribution. For the spectral/ $hp$  element solver in space, four elements are used in the domain, as shown in Fig. 17. Within each mesh, 10th-order (Jacobi) polynomials are employed. In the random space, the third-order Legendre-chaos, corresponding to the uniformly

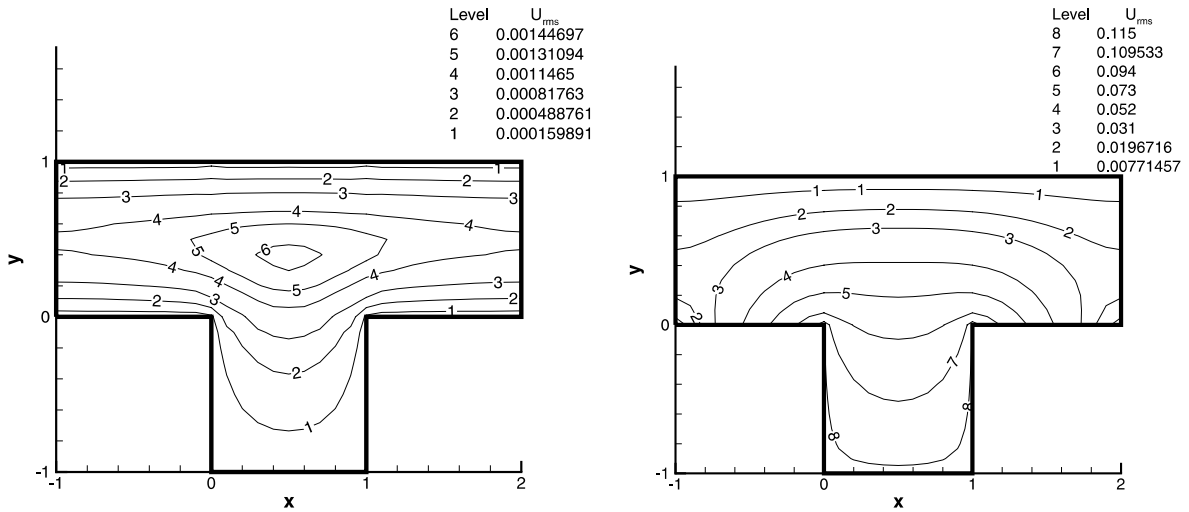


Fig. 18. Standard deviations of heat conduction in the grooved channel; left: solution subject to random diffusivity only; right: solution subject to random diffusivity and random boundary conditions.

distributed random inputs, is used. Resolution checks indicate that the above discretization is sufficient to resolve the problem, both in physical and random spaces.

We consider two cases: the first case is when only the diffusivity  $\kappa$  is random, while the boundary condition along  $\Gamma_C$  is deterministic, i.e.,  $u|_{\Gamma_C} = 1$ . Same as in section 4.2.1, the first four eigenmodes of the KL decomposition are employed to represent  $\kappa$ . This results in a four-dimensional ( $n = 4$ ) chaos expansion. For third-order chaos ( $p = 3$ ), a total of 35 expansion terms are needed from (23). In the second case, we further assume the boundary condition along the wall of cavity  $\Gamma_C$  is random as in (42), and is independent of the random field  $\kappa$ . This introduces one more dimension in the random space and a total of 56 expansion terms are needed for third-order chaos expansion;  $n = 5$ ,  $p = 3$  from (23).

In Fig. 18, the contours of the standard deviations of the solution are plotted. The solution of the first case is shown on the left, while solution of the second case on the right. In both cases, the standard deviations of the random inputs are  $\sigma = 0.2$ . No noticeable difference is observed between the mean solutions of the two cases, and that of the corresponding deterministic case. However, the standard deviations of the solutions are very different for the two cases. From Fig. 18, we can see that the effect of uncertainty in the diffusivity is subdominant (maximum deviation about only 0.15%). By introducing the uncertainty in boundary condition along the walls of the cavity, the output uncertainty is greatly enhanced in the entire domain (maximum deviation about 12%), and its structure is changed; the maximum of the output uncertainty moves from the center of the channel to the lower wall of the cavity.

## 5. Summary

We have developed a stochastic spectral method to model uncertainty in steady state diffusion problems. The generalized polynomial chaos we introduced includes the original polynomial chaos, the Hermite-chaos, as a subset, and is an extension of the original chaos idea of Wiener [12] and of the work of Ghanem and Spanos [11]. The important feature of the new broader framework is that it incorporates different types of chaos expansion corresponding to several important distribution functions, including some discrete distributions which cannot be readily handled by the original polynomial chaos directly.

We have applied the generalized polynomial chaos to the solution of steady state random diffusion problems, as a natural extension of our earlier work [17,19,20]. In particular, we employed a block Gauss–Seidel iteration technique to solve the system of equations efficiently. An ‘elementary’ correlation function in two dimensions, the Bessel correlation function, was studied and applied in the computations. The KL decomposition is used to reduce the dimensionality of the random space.

We have shown that, when the appropriate chaos expansion is chosen according the random input, the generalized polynomial chaos solution converges exponential fast due to the fact that it is a spectral expansion in the random space. The exponential convergence rate is demonstrated for one-dimensional model problem, and is in accordance with the result of [17]. For more complicated problems, the Monte Carlo simulation is employed to validate the chaos solution. We observe good agreement between the well-resolved chaos expansion solution and the converged Monte Carlo simulation results. For this particular problem, tens of thousands realizations are needed for the Monte Carlo computation, and the generalized polynomial chaos expansion is at least two to three orders faster. In particular, we confine our applications to problems within finite domain in the physical space. Fast convergence of the chaos expansion is observed with relatively large variance of the random input. Problems with infinite physical domain require separate treatment.

The efficiency of the chaos expansion is problem specific and depends greatly upon the dimensionality of the random space. Although KL decomposition, among other possible techniques, can be used to reduce the dimensionality, it can be large for systems with very short correlation length, e.g., the white noise. To this end, the number of expansion terms may be very large, thus reducing the efficiency of the chaos expansion drastically. This problem also deserves further research.

## Acknowledgements

This work was supported by ONR and DOE. Computations were performed at Brown’s TCASCV and NCSA’s (University of Illinois) facilities.

## References

- [1] Workshop on Validation and Verification of Computational Mechanics Codes, Technical report, Caltech, December 1998.
- [2] Workshop on Predictability of Complex Phenomena, Los Alamos, 6–8 December, 1999, Technical report.
- [3] Workshop on Decision Making Under Uncertainty, IMA, 16–17 September, 1999, Technical report.
- [4] W.L. Oberkampf, T.G. Trucano. Validation methodology in computational fluid dynamics. Technical Report AIAA 2000-2549, Sandia National Laboratories, Albuquerque, New Mexico, 2000.
- [5] W.K. Liu, T. Belytschko, A. Mani, Random field finite elements, *Int. J. Numer. Meth. Engrg.* 23 (1986) 1831–1845.
- [6] W.K. Liu, T. Belytschko, A. Mani, Probabilistic finite elements for nonlinear structural dynamics, *Comput. Meth. Appl. Mech. Engrg.* 56 (1986) 61–81.
- [7] W.K. Liu, T. Belytschko, A. Mani, Applications of probabilistic finite element methods in elastic/plastic dynamics, *J. Engrg. Ind., ASME* 109 (1987) 2–8.
- [8] M. Kleiber, T.D. Hien, *The stochastic finite element method*, Wiley, 1992.
- [9] F. Yamazaki, M. Shinozuka, G. Dasgupta, Neumann expansion for stochastic finite element analysis, Technical report, Department of Civil Engineering, Columbia University, 1985.
- [10] M. Shinozuka, G. Deodatis, Response variability of stochastic finite element systems, Technical report, Department of Civil Engineering, Columbia University, New York, 1986.
- [11] R.G. Ghanem, P. Spanos, *Stochastic Finite Elements: a Spectral Approach*, Springer, 1991.
- [12] N. Wiener, The homogeneous chaos, *Amer. J. Math.* 60 (1938) 897–936.
- [13] R.G. Ghanem, Ingredients for a general purpose stochastic finite element formulation, *Comp. Meth. Appl. Mech. Engrg.* 168 (1999) 19–34.
- [14] A.J. Chorin, Hermite expansion in Monte-Carlo simulations, *J. Comput. Phys.* 8 (1971) 472–482.

- [15] M.K. Deb, I.M. Babuška, J.T. Oden, Solution of stochastic partial differential equations using Galerkin finite element techniques, *Comput. Meth. Appl. Mech. Engrg.* 190 (2001) 6359–6372.
- [16] R.H. Cameron, W.T. Martin, The orthogonal development of nonlinear functionals in series of Fourier–Hermite functionals, *Ann. Math.* 48 (1947) 385.
- [17] D. Xiu, G.E. Karniadakis, The Wiener–Askey polynomial chaos for stochastic differential equations, *SIAM J. Sci. Comput.*, in press.
- [18] R. Askey, J. Wilson, Some basic hypergeometric polynomials that generalize Jacobi polynomials, *Mem. Amer. Math. Soc.*, AMS Providence, RI 319 (1985).
- [19] D. Xiu, G.E. Karniadakis, Modeling uncertainty in flow simulations via generalized polynomial chaos, *J. Comput. Phys.*, in press.
- [20] D. Xiu, D. Lucor, C.-H. Su, G.E. Karniadakis, Stochastic modeling of flow-structure interactions using generalized polynomial chaos, *J. Fluid Engrg.* 124 (2002) 51–59.
- [21] I. Babuška, On randomized solutions of Laplace’s equation, *Casopis Pest. Mat.* 36 (1961) 269–276.
- [22] G.A. Bécus, F.A. Cozzarelli, The random steady state diffusion problem. I. Random generalized solutions to Laplace’s equation, *SIAM J. Appl. Math.* 31 (1976) 134–147.
- [23] G.A. Bécus, F.A. Cozzarelli, The random steady state diffusion problem. II. Random solutions to nonlinear inhomogeneous, steady state diffusion problems, *SIAM J. Appl. Math.* 31 (1976) 148–158.
- [24] G.A. Bécus, F.A. Cozzarelli, The random steady state diffusion problem. III. Solutions to random diffusion problems by the method of random successive approximations, *SIAM J. Appl. Math.* 31 (1976) 159–178.
- [25] G.C. Papanicolaou, Diffusion in random media, in: J.B. Keller, D. McLaughlin, G.C. Papanicolaou (Eds.), *Surveys in Applied Mathematics*, Plenum Press, 1995, pp. 205–255.
- [26] H. Holden, R. Oksendal, J. Ubøe, T. Zhang, *Stochastic Partial Differential Equations: A Modeling, White Noise Functional Approach*, Birkhäuser, Boston, 1996.
- [27] H.G. Matthies, C. Bucher, Finite elements for stochastic media problems, *Comput. Meth. Appl. Mech. Engrg.* 168 (1999) 3–17.
- [28] W. Schoutens, *Stochastic Processes and Orthogonal Polynomials*, Springer, New York, 2000.
- [29] R. Koekoek, R.F. Swarttouw, The Askey-scheme of hypergeometric orthogonal polynomials and its  $q$ -analogue, Technical Report 98-17, Department of Technical Mathematics and Informatics, Delft University of Technology, 1998.
- [30] N. Wiener, *Nonlinear Problems in Random Theory*, MIT Technology Press and Wiley, New York, 1958.
- [31] H. Ogura, Orthogonal functionals of the Poisson process, *IEEE Trans. Info. Theory* IT-18 (1972) 473–481.
- [32] M. Loève, *Probability Theory*, fourth ed., Springer, 1977.
- [33] G.E. Karniadakis, S.J. Sherwin, *Spectral/hp Element Methods for CFD*, Oxford University Press, 1999.
- [34] M. Anders, M. Hori, Three-dimensional stochastic finite element method for elasto-plastic bodies, *Int. J. Numer. Meth. Engrg.* 51 (2001) 449–478.
- [35] P. Whittle, On stationary processes in the plane, *Biometrika* 41 (1954) 434–449.